Available online at www.sciencedirect.com
SCIENCE DIRECT®
ELSEVIER
Nuclear Instruments and Methods in Physics Research A 503 (2003) 567–579
NUCLEAR INSTRUMENTS & METHODS IN PHYSICS RESEARCH Section A
www.elsevier.com/locate/nima

WITCH: a recoil spectrometer for weak interaction and nuclear physics studies

M. Beck[a,*], F. Ames[b], D. Beck[c], G. Bollen[d], B. Delauré[a], V.V. Golovko[a], V.Yu. Kozlov[a], I.S. Kraev[a], A. Lindroth[a], T. Phalet[a], W. Quint[c], P. Schuurmans[a,1], N. Severijns[a], B. Vereecke[a], S. Versyck[a]

[a] *Instituut voor Kern- en Stralingsfysica, K.U.Leuven, Celestijnenlaan 200D, B-3001 Leuven, Belgium*
[b] *Ludwig-Maximilians-Universität, Sektion Physik, Schellingstraße 4/IV, D-80799 München, Germany*
[c] *GSI-Darmstadt, Planckstr. 1, D-64291 Darmstadt, Germany*
[d] *NSCL/Michigan State University, East Lansing, MI 48824, USA*

The ISOLDE EUROTRAPS and NIPNET Collaborations

Received 25 November 2002; received in revised form 4 February 2003; accepted 6 February 2003

Abstract

An experimental set-up is described for the precise measurement of the recoil energy spectrum of the daughter ions from nuclear beta decay. The experiment is called WITCH, short for Weak Interaction Trap for CHarged particles, and is set up at the ISOLDE facility at CERN. The principle of the experiment and its realization are explained as well as the main physics goal. A cloud of radioactive ions stored in a Penning trap serves as the source for the WITCH experiment, leading to the minimization of scattering and energy loss of the decay products. The energy spectrum of the recoiling daughter ions from the β-decays in this ion cloud will be measured with a retardation spectrometer. The principal aim of the WITCH experiment is to study the electroweak interaction by determining the beta-neutrino angular correlation in nuclear β-decay from the shape of this recoil energy spectrum. This will be the first time that the recoil energy spectrum of the daughter ions from β-decay can be measured for a wide variety of isotopes, independent of their specific properties.
© 2003 Elsevier Science B.V. All rights reserved.

PACS: 23.40.Bw; 29.30; 39.10

Keywords: Weak interaction; Beta decay; Scalar interaction; Ion trap; Penning trap; Retardation spectrometer

1. Introduction

The standard model of the electroweak interaction is very successful in describing the interaction both qualitatively and quantitatively. However, it contains many free parameters and ad hoc

*Corresponding author. Tel.: +32-16-327265; fax: +32-16-327985.
E-mail address: marcus.beck@fys.kuleuven.ac.be (M. Beck).
[1] Present address: SCKCEN, Belgian Nuclear Research Center, Boeretang 200, B-2400 Mol, Belgium.

0168-9002/03/$ - see front matter © 2003 Elsevier Science B.V. All rights reserved.
doi:10.1016/S0168-9002(03)00994-X

assumptions. One of these is that from the five possible types of weak interactions—vector (V), axial-vector (A), scalar (S), tensor (T) and pseudoscalar interaction (P)—just V and A interactions are present at a fundamental level. Together with maximal parity violation this has led to the well known V–A structure of the weak interaction. Most experimental limits for the S and T coupling constants in the charged current sector are rather weak, though [1–4], i.e. of the order of 10% of the coupling constants of V and A interactions, corresponding to the exchange of a boson of mass $m_{\text{boson}} \approx 300$ GeV when standard coupling is assumed. Only the limits on neutral current S and T interactions are very stringent [5]. Experiments in all three sectors of the weak interaction, i.e. the leptonic, semileptonic and hadronic sectors, can search for S and T interactions. They yield complementary information when the exclusion of specific particle models, such as leptoquarks [1,6], is considered.

In order to improve the limits on S and T interactions the WITCH experiment intends to measure the beta-neutrino angular correlation in nuclear beta decay [7], ω, with high precision:

$$\omega_{(\vartheta_{\beta\nu})} \sim 1 + a \cdot \frac{v}{c} \cdot cos(\vartheta_{\beta\nu}) \cdot \left(1 - b \cdot \frac{\Gamma \cdot m}{E}\right). \qquad (1)$$

Here $\vartheta_{\beta\nu}$ is the angle between the emitted β-particle and the neutrino, and a the β-ν angular correlation coefficient. Further v/c, m and E represent velocity, rest mass and total energy of the β-particle, while $\Gamma = \sqrt{(1-(\alpha \cdot Z)^2)}$ with α the fine-structure constant and Z the nuclear charge of the daughter nucleus. The Fierz interference coefficient b has experimentally been shown to be small [8–11] and will be assumed to be zero in the following discussion.

From the properties of the general Hamiltonian of the weak interaction [12] and the Dirac γ-matrices it can be shown that V interaction only takes place between a particle and an antiparticle with opposite helicities and S interaction only between a particle and an antiparticle with the same helicity. Therefore in super-allowed $0^+ - 0^+$ Fermi decays, where the β- and neutrino spins have to couple to zero, particle and antiparticle will be emitted preferentially into the same direction for V interaction and into opposite directions for S interaction. On average this will lead to a relatively large recoil energy for V interaction (Fig. 1) and a relatively small recoil energy for S interaction. For pure Fermi decays the dependence of a on the interaction type is [7]

$$a = \frac{2 - |\tilde{C}_S|^2 - |\tilde{C}'_S|^2 + 2 \cdot Z \cdot \alpha \cdot m/p \cdot Im(\tilde{C}_S + \tilde{C}'_S)}{2 + |\tilde{C}_S|^2 + |\tilde{C}'_S|^2} \qquad (2)$$

with $\tilde{C}_S = C_S/C_V$ and $\tilde{C}'_S = C'_S/C'_V$, where C_S and C_V and their primed counterparts are the coupling constants for S and V interactions, respectively [12,13].

In super-allowed Fermi transitions only V interaction can contribute to the decay rate according to the Standard Model. From Eq. (2) it then follows that $a = 1$. Any admixture of S to V interaction in such a transition would result in $a < 1$. By measuring the β-ν angular correlation coefficient a one can thus determine which interactions contribute.

Since the neutrino cannot be detected directly in such an experiment the β-ν angular correlation has to be inferred from other observables like the shape of the β- or recoil energy spectrum. Angular correlation experiments of this kind have previously established the predominant V–A character of the electroweak interaction [3,4,14,15].

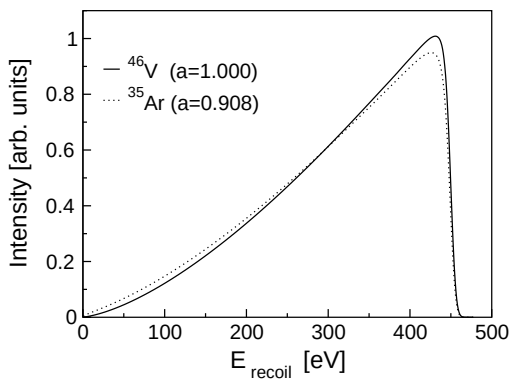

Fig. 1. Calculated differential recoil energy spectra for $a = 1$ (^{46}V) and $a = 0.908$ (^{35}Ar). The energy axis of the spectrum of ^{46}V has been scaled in order to have the same endpoint energies for both spectra. The experiment discussed in this article intends to distinguish between $a = 1$ and 0.995.

However, these experiments are difficult since the β-emitter is usually embedded in matter, e.g. an ion catcher, which will cause a distortion of the spectra due to energy losses. Indeed, the β-particles will be scattered and, in most cases, the recoiling daughter nuclei will be fully stopped in the source due to their very low kinetic energy, usually of the order of just a couple of hundred eV. Consequently, the β-ν angular correlation has been measured in just a few exceptional cases up to now [3,4,14,15].

The early recoil experiments, e.g. References [14,15] were restricted to gases. They used a gaseous source, thus reducing the problem of scattering. The isotopes for which the recoil energy spectrum was measured directly are ^{6}He, ^{19}Ne, ^{23}Ne, and ^{35}Ar. The precision which these experiments reached for a was $\Delta a \geqslant 0.04$. This was sufficient to determine the predominant V–A character of the electroweak interaction [15]. The most precise determination of a was achieved recently with ^{32}Ar [3,4]. Here the activity was implanted into a thin carbon foil. After the β-decay of ^{32}Ar the daughter isotope ^{32}Cl decays via proton emission. This happens sufficiently fast so that the recoiling daughter ion does not scatter in the carbon catcher. The proton leaves the foil due to its much higher energy (O(MeV)) compared to the recoil ion (O(100eV)). a is then determined indirectly from the Doppler broadening of the proton due to the recoil. This experiment has yielded the most precise determination of a up to now with $\Delta a_{\mathrm{stat}} = 0.0052$ and $\Delta a_{\mathrm{sys}} = 0.0039$. In the WITCH experiment scattering of the recoil ions will be avoided by using a Penning trap. In such a Penning trap the ions are stored in vacuum. This eliminates any energy loss caused by the matter that usually surrounds the radioactive source ions or atoms.

With the WITCH experiment it is intended to reach a similar precision on a in a systematic measurement of several superallowed Fermi-decay and eventually improve the precision even further. In addition, also Gamow–Teller β-decays, which are sensitive to tensor type weak interactions and for which the best experiment has reached a precision of just $\Delta a \approx 0.01$, will be addressed. Finally, the WITCH experiment allows to determine a number of nuclear structure related observables such as e.g. Fermi/Gamow–Teller mixing ratios and Q_{EC}-values.

2. The experiment

2.1. Principle

In order to avoid that the recoiling daughter ions are stopped in the source, and to be as independent on the properties of the isotopes as possible, the WITCH experiment will utilize a Penning trap to store the radioactive ions. A Penning trap is an electromagnetic ion trap. It combines a high magnetic field, which constrains the ion motion radially, with an electrostatic quadrupole potential, which constrains it axially [16,17]. The radioactive ions then form an ion cloud in vacuum in the center of the Penning trap. After β-decay the recoiling daughter ions have kinetic energies in the range $0 \leqslant E_{\mathrm{recoil}} \leqslant O(100\ \mathrm{eV})$. Those recoil ions with axial energy larger than the trap potential (O(10 V)) will leave the trap. Due to the low density of the ion cloud (typically $\leqslant 10^{7}$ ions/cm^{3}) they experience no significant energy loss. The open cylindrical structure of the Penning trap used (see Section 2.2) then allows the recoil ions to leave the trap without scattering off the trap electrodes. Consequently, the ions leave the trap with the full recoil energy from the β-decay.

The Penning trap is placed at the entrance of a retardation spectrometer. The recoil ions emitted into the direction of the spectrometer spiral from the trap, which is situated in a magnetic field of $B_{\mathrm{max}} = 9$ T, to a region where the magnetic field reaches a plateau of $B_{\mathrm{min}} = 0.1$ T. Provided that the fields change sufficiently slowly along the path of the ions, their motion can be considered to be adiabatic. Then, according to the principle of adiabatic invariance of the magnetic flux contained in the ion motion [18], i.e. of the magnetic moment of the ion motion, a fraction of

$$1 - B_{\mathrm{min}}/B_{\mathrm{max}} \approx 98.9\% \tag{3}$$

of the radial energy of the ions gets converted into axial energy while the ions spiral from the high to the low magnetic field region. Due to an electrostatic retardation potential U_{ret} that is applied

between the trap and the low-field region only ions with axial energy

$$E_{\text{axial}} > n \cdot e \cdot U_{\text{ret}} \quad (4)$$

can pass this analysis region; n is the charge state of the ion and e the elementary charge. By counting how many ions pass the analysis plane for different retardation potentials, the cumulative recoil energy spectrum can be measured. This is the same fundamental principle that is used in the experiments to determine the mass of the electron anti-neutrino in Mainz [19,20] and Troitsk [21].

Besides the WITCH experiment there are other trap experiments under development in which it is intended to measure the recoil energy spectrum after β-decay. They are either specific to one isotope [22] or use a magneto-optic trap (MOT, an atom trap [23–25]), which is limited to elements with suitable optical transitions. A Penning trap was chosen for WITCH since Penning traps, like Paul traps, are not limited to trapping of specific elements, and the isotope that is best suited for a given purpose can be chosen freely. In order to fully utilize this property the WITCH experiment is being installed at the ISOLDE facility at CERN [26,27] where a wide variety of different isotopes is available at high intensities. Thus the WITCH experiment opens a universal way to study β-decay via the energy spectrum of the daughter nucleus [28–35]. For the first time it will be possible to measure this observable independent of the chemical, atomic or decay properties of the isotopes in question. For the search for S and T weak interactions this means that the most suitable β-emitters, decaying either via a pure Fermi or a pure Gamow–Teller transition, can be selected.

2.2. Set-up

An overview of the experimental set-up is shown in Fig. 2. In a first step the ions produced by ISOLDE get trapped and cooled by REXTRAP [36], a Penning trap, which serves to bunch, cool and purify the ion beams for the REX-ISOLDE project. When the ions are transmitted from REXTRAP to the WITCH experiment they pass through a horizontal beamline into an electrostatic 90° bender with spherical electrodes, where they

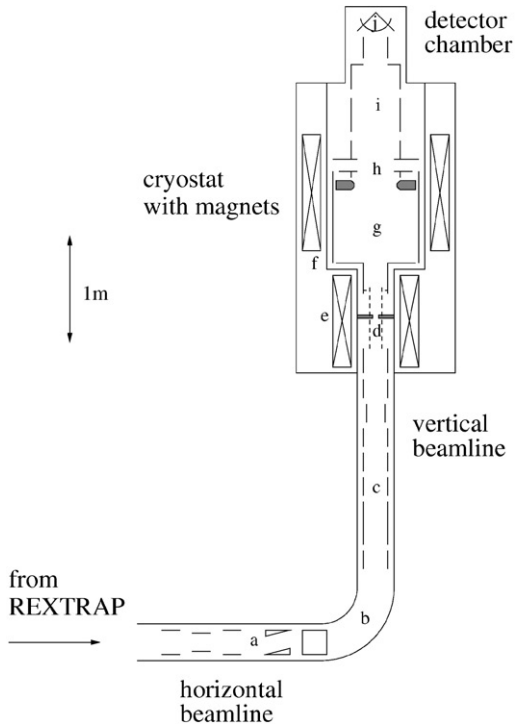

Fig. 2. The experimental set-up consists of several parts: a horizontal beamline (a), which is connected via a spherical 90° bender (b) to a vertical beamline (c). Both beamlines contain electrostatic ion optics, e.g steerers and an Einzel lens in the horizontal beamline and retardation electrodes as well as a pulsed drift tube in the vertical beamline. Two Penning traps (d) are located in the bore of a 9 T magnet (e). The retardation spectrometer is formed by this magnet, a 0.1 T magnet (f) and retardation electrodes (g). Finally, the set-up contains an electrostatic acceleration section (h), a large Einzel lens (i) and an ion detector (j). For details of the Penning traps and the retardation spectrometer see Figs. 3 and 5. This figure is only approximately to scale.

are deflected upward into the vertical beamline. There the ions are electrostatically decelerated from 60 keV to 50 eV in several steps. In order to avoid a high-voltage platform for the spectrometer the potential of the ions relative to ground must be changed. This is achieved by using a drift tube that is located in the vertical beamline and is pulsed by 60 kV while the ions are inside [37].

2.2.1. Penning traps

The Penning trap has to capture, cool, center and store the ions. In order to separate these

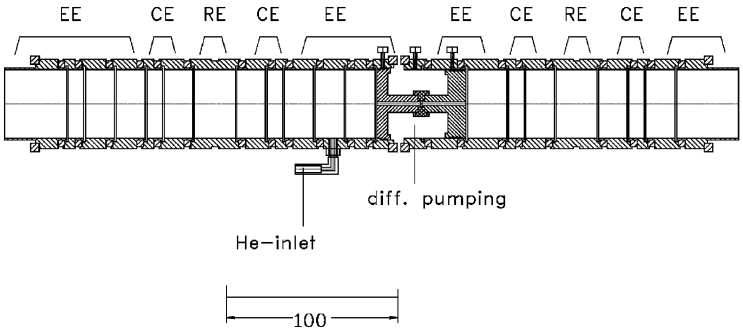

Fig. 3. Geometry of the Penning traps. The cooler trap (left) is separated from the decay trap (right) by a differential pumping barrier. The inner diameter of the trap electrodes is 4 cm. The distance between the trap centers is 21.1 cm and the total length of the two traps 42.8 cm. *EE* denotes the end-cap electrodes, *CE* the correction electrodes and *RE* the central ring electrode of the traps. The buffer gas inlet is also indicated.

functions two Penning traps are used, a cooler trap and a decay trap (Fig. 3). Both have cylindrical electrodes with an inner diameter of 4 cm. The electrodes are made of gold-plated oxygen-free copper and are separated by insulators made of the glass ceramic Macor.[2] The ions get trapped in the cooler trap first. This trap is a copy of the cooler trap of the ISOLTRAP experiment [38–40]. It consists of seven cylindrical electrodes—the central ring electrode, two pairs of correction electrodes and two end-cap electrodes. The latter are longitudinally split into four segments each. The electrodes form a nested trap with two potential wells, the first of which is defined by the ring, correction and innermost end-cap electrodes, which create the usual quadrupole potential. The second potential well is box like and is created by the remaining outer end-cap electrodes. It is used to initially trap the ions by buffer gas assisted dynamic capture. For this purpose helium gas is injected into the trap as buffer gas in order to dampen and cool the ion motion [41]. In addition, the ring electrode is azimuthally divided into eight and the inner correction electrodes into four identical segments. This azimuthal segmentation allows for manipulation of the ions with radio-frequency fields, which is needed to cool and center the ions.

After the ions are trapped a mass-selective cooling technique is applied which brings the trapped ions to approximately room temperature [42]. In this process the ions lose energy due to collisions with buffer gas atoms. This will cool all three motions of the ions in the trap, i.e. the reduced cyclotron, the magnetron and the axial motion. However, since the radius of the magnetron motion increases for decreasing magnetron energy the ions need to be recentered. This is achieved by applying an azimuthal radio-frequency quadrupole field to the central ring electrode at the true cyclotron frequency of the trapped ions, which couples the magnetron and the reduced cyclotron motion. In combination with the buffer gas cooling the ions will be mass-selectively centered in the trap after a time of several ms to s, depending on the parameters chosen. The resulting ion cloud will have a radial and axial size of several mm (for 10^7 ions, [43]). Subsequently the cooled and centered ions are ejected through the opening in a differential pumping barrier into the second Penning trap, the decay trap, which is a modified version of the cooler trap. The ions are stored here for approximately one half-life, typically 1–10 s for the cases of interest. The ion cloud in the decay trap constitutes the source for the experiment.

Similar to the cooler trap the decay trap consists of seven electrodes. However, since the decay trap just has to capture a short ion pulse of a low, well defined energy, the use of buffer gas and a box-like outer potential well are not necessary. Therefore the decay trap is shorter than the cooler trap and the end-cap electrodes are split into two rather than four different segments each.

[2] Macor is a registered trademark of Corning Inc.

Both Penning traps are operated in the room-temperature bore of the same superconducting magnet. The inner bore diameter is ≈ 130 mm and the magnetic field strength $B_{max} = 9$ T (Figs. 4, 5). The homogeneity of the magnetic field is $\Delta B/B = 4 \times 10^{-6}$ in a region of length 30 mm and diameter 10 mm in the center of the cooler trap and $\Delta B/B = 8 \times 10^{-6}$ in a region of length 30 mm and diameter 10 mm in the center of the decay trap.

The traps get pumped, together with the spectrometer, by two 900 l/s turbo pumps (helium pumping speed), one close to the cooler trap, the other at the opposite end of the spectrometer. The system is designed to reach a pressure of $< 10^{-9}$ mbar without buffer gas in both traps. Under normal operating conditions the helium partial pressure needed for the capture and buffer gas cooling of the ions in the cooler trap is in the range 10^{-6} to 10^{-3} mbar. In contrast, the rest gas pressure needs to be as low as possible in the decay trap to achieve long storage times. In order to accommodate both requirements a differential pumping barrier with inner diameter of 2–3 mm is situated between the two traps. The length of this barrier can be varied from 2.5 to 5 cm. It has to provide for a pressure reduction of a factor of 10^2–10^3 in order to yield a helium partial pressure of $\leqslant 10^{-6}$ mbar in the decay trap (see also Section 3.4). The optimum parameters for the differential pumping barrier will be determined during the initial phase of the experiment.

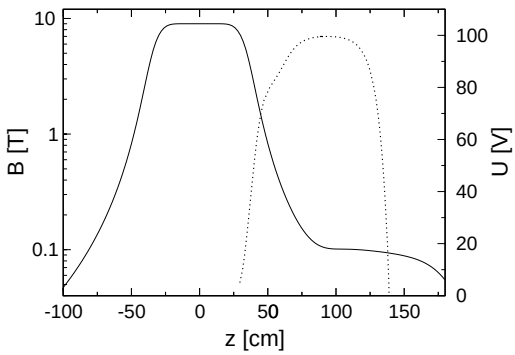

Fig. 4. Magnetic (solid line) and electric (dashed line) fields on the axis of the retardation spectrometer. The two Penning traps are in the region with $B = 9$ T. The electric field has been calculated for $U_{ret} = 100$ V. The trap potential is not shown.

2.2.2. Spectrometer

The decay trap is located at the entrance of the retardation spectrometer (Fig. 5). The recoiling daughter ions from the β-decays in this trap are emitted isotropically with kinetic energies of typically $E_{recoil} < 500$ eV. Those ions emitted with a velocity component in the direction of the cooler trap are lost in the initial version of the experiment; at a later stage an electrostatic mirror will be used to reflect them into the opposite direction. Those ions emitted towards the spectrometer spiral from the decay trap where the magnetic field is $B_{max} = 9$ T to the analysis region where the magnetic field reaches a plateau of $B_{min} = 0.1$ T.

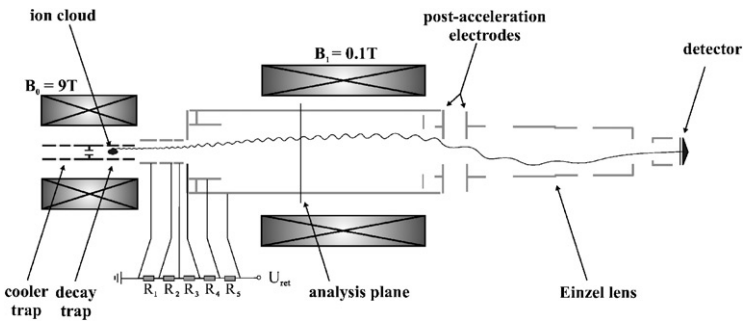

Fig. 5. Spectrometer section of the experimental set-up. The two Penning traps are located in the region with $B = 9$ T. The retardation electrodes are in the region between the end of the decay trap and the end of the low-field magnet. The electrode configuration shown is consistent with the requirements as discussed in Sections 2.1 and 2.2.2 and has been optimized as discussed in Section 3.4. The retardation potential reaches its maximum in the homogeneous field region of the 0.1 T magnet. Then follow a screening electrode and the electrodes for postacceleration. Finally, the Einzel lens focuses the ions onto the detector.

This low-field region is created by a second superconducting magnet with an inner bore diameter of 420 mm. It shares a common cryostat with the 9 T magnet. This magnet system was built by Oxford Instruments Ltd.

Between the trap and the analysis region are several cylindrical retardation electrodes. The retardation potential increases for each electrode until it reaches its maximal value at the electrode surrounding the analysis region (Figs. 4, 5). A possible sequence of potentials applied to the electrodes is shown in Table 1. The values for the intermediate potential steps were chosen so as to avoid steep gradients in the potential. The gradient of the resulting electric potential points approximately in the direction of the magnetic field. Both the absence of steep gradients in the electric and magnetic fields and the approximate alignment of these fields are necessary to achieve adiabatic conversion of radial into axial kinetic energy [19].

The ions that pass the retardation potential in the analysis region get immediately accelerated by another electrostatic potential of $U_{acc} \approx -10$ kV that is applied to a set of postacceleration electrodes. This is necessary in order that the ions get nonadiabatically off the magnetic field lines instead of following them. Finally, the ions are focused with an Einzel lens onto the detector, which is at a potential of ≈ -10 kV to provide for sufficient energy of the ions in order that their detection efficiency is independent of their kinetic energy. Electrostatic focusing rather than magnetic focusing with another high-field magnet was preferred for two reasons. First, simulations showed that it would be very difficult to focus the retarded ions magnetically without losing some of them due to a magnetic mirror effect. Second, the reflected ions as well as positrons in the case of β^+-decays would accumulate in the magnetic bottle created by the two magnets and create a space charge, which would alter the electric potentials in the spectrometer.

Table 1
Percentage of the retardation potential U_{ret} that is applied to the retardation electrodes of the spectrometer. U_{ret} is with respect to the central ring electrode of the decay trap which is on ground potential

Electrode	Voltage in % of U_{ret}
1	0
2	30
3	60
4	80
5	80
6	100

Initially, a microchannel plate detector will be used to detect the recoil ions. This type of detector can detect individual ions at low kinetic energies ($\geqslant 2$ keV, [44]). In order to determine whether all ions reach the detector its anode is segmented radially. If the outermost segment shows no counts in excess of the background it can be assumed that all ions are focused onto the detector. By measuring the count rate for different retardation potentials the cumulative energy spectrum of the daughter ions will be determined.

The retardation spectrometer has to fulfill several conditions in order to precisely measure the recoil energy spectrum. First, simulations showed that its resolution needs to be $O(1\%)$ or better in order to achieve the required precision on a of $\Delta a = 0.005$. Second, the spectrometer needs to be able to handle recoil ions from β-decays with Q-values of up to $Q \approx 7$ MeV at $A \approx 50$. An example of such a high-energy case is ^{46}V. Third, the transmission of ions from the trap to the detector must be close to 100%. It is important that this transmission efficiency does not significantly depend on the kinetic energy of the recoil ions. This implies that all transmitted ions have to be focused onto a detector with a spot size of around 2 cm in diameter, independently of their kinetic energy, their emission angle and the size of the ion cloud. Finally, the measured response function of the spectrometer should deviate as little as possible from the ideal response function, which can be calculated analytically. Any such deviation will provide clues to imperfections of the performance of the spectrometer.

In order to achieve these goals it must be known how the ion trajectories behave for a specific combination of electric and magnetic fields. Then, the electric field created by the electrodes as well as the design of the magnet can be optimized. Most importantly, the magnetic and electric fields have

to be shaped in a manner that allows for adiabatic motion of the ions.

The design of the spectrometer was an iterative process. In a first step a preliminary magnetic field configuration was chosen. Then a tentative electrode arrangement was determined, taking into account the magnetic field plot for that magnet configuration. The potential of each electrode was determined by a relaxation method, respecting the boundary conditions imposed by the other electrodes. A Stokes force was added to the equation of motion in order to simulate the dampening of the ion motion by buffer gas. In a next step a set of ions having a monochromatic energy and isotropic emission was placed in an ion cloud in the center of the trap. The ion trajectories from the trap to the detector were then obtained by solving the equation of motion numerically using a 5th order Runge Kutta method with adaptive step size (adopted from [45]). This calculation was repeated varying the spatial distribution of the ion cloud in the trap, the kinetic energy and mass of the ions and the retardation voltage of the spectrometer. Typically around 10^8 trajectories were calculated for a given spectrometer configuration. The last step consisted of obtaining the spot size at the detector, the response function and, in some cases, the number of lost ions. As a result, the properties of the spectrometer were obtained for a given spectrometer configuration. This process was repeated for different arrangements of electrodes and magnets in order to maximize the transmission of the spectrometer and to get the best possible resolution. Other boundary conditions have been the technical feasibility, the space available in the experimental hall of ISOLDE as well as the cost of the spectrometer. The magnet configuration was developed in collaboration with Oxford Instruments Ltd. and Magnex Scientific Ltd. taking into account that the magnets should be available 'off the shelf' and the field of the high-field magnet should not exceed 9 T for price reasons.

The spectrometer as presented in this paper is the result of the procedure described above. In the calculations it fulfills all requirements. An energy resolution of 1.2% is obtained even for the high Q-value decay of ^{46}V.

3. Operational characteristics

3.1. Normalization

The number of ions in the decay trap can vary from one trap load to another. Therefore a suitable method to determine the initial number of ions in each trap load needs to be applied for normalization. One way consists of counting the number of ions that are left in the trap after a certain time. For this purpose the stored ions can be ejected from the trap onto a normalization counter. If the storage time in the decay trap is the same for all trap loads, the number of ions counted by the microchannel plate detector can be normalized to the number of ions detected by the normalization counter. Alternatively, by extrapolating to the time the trap was filled the initial trap load can be determined and used for normalization. Another method utilizes the β-particles that are emitted together with the recoil ions. Since they have a similar momentum as the recoil ions they also follow the magnetic field lines. However, since the energy of the β-particles is much larger than the potential that the final Einzel lens creates ($E_\beta = O(\text{MeV})$ whereas $U_{\text{Einzel}} \approx 10$ kV), the β-particles will not be focused onto the detector. When following the magnetic field lines most of them will eventually hit the electrodes mounted in the vacuum chamber or the chamber walls. In order to detect some of these β-particles for normalization purposes a β-detector will be installed in the spectrometer. The number of β-particles that are counted with this detector is a measure of the total number of ions present in the trap.

A small fraction of the β-particles will still reach the detector and thus induce a flat background in the cumulative recoil energy spectrum since $|E_\beta| \gg |e \cdot U_{\text{ret}}|$ on average. It is expected that this background amounts to several percent of the decay rate.

3.2. Charge states

The daughter ions from β-decay can have different charge states $q = n \cdot e$ due to electron shake-off [46]. Therefore recoil ions with kinetic

energy E_{recoil} and charge q will appear in the measured spectrum at a retardation voltage $U_{\mathrm{ret}} = E_{\mathrm{recoil}}/q$. The measured spectrum will thus be a superposition of the spectra of the various charge states, each with different endpoints $U_{0n} = E_0/(n \cdot e), n \geqslant 1$, where $E_0 = (\Delta^2 - m_{\mathrm{e}}^2)/2 \cdot m_{\mathrm{i}}$ is the endpoint energy of the recoil energy spectrum. Here m_{i} (m_{f}) and E_{i}^* (E_{f}^*) are the mass and the excitation energy of the parent (daughter) ion, m_{e} is the electron mass, $\Delta = Q - m_{\mathrm{e}}$ and $Q = m_{\mathrm{i}} - m_{\mathrm{f}} + E_{\mathrm{i}}^* - E_{\mathrm{f}}^*$ is the Q-value of the decay. Consequently, when measuring the full recoil spectrum up to the endpoint energy E_0, the upper half of the spectrum will consist purely of events from charge state $n = 1$. Between $E_0/2$ and $E_0/3$ both charge states $n = 1$ and 2 will be present, between $E_0/3$ and $E_0/4$ charge states $n = 1$ to 3, etc. By restricting the measurement or the analysis to the upper half of the spectrum a clean spectrum of charge state $n = 1$ can be obtained.

3.3. Energy calibration

The energy calibration of the recoil energy spectrum can be obtained in various ways. The simplest possibility is to use the potentials that are applied to the retardation electrodes, which can be measured precisely. However, the potential that the ions experience may not be exactly the same as the potential that is applied to the electrodes. An alternative possibility to perform the energy calibration is given by electron-capture decay (EC), which always accompanies β^+-decay, albeit at a possibly very small branching ratio. EC-decay leaves two particles in the final state, the recoil ion and a neutrino. Due to energy- and momentum conservation both particles are monoenergetic, i.e. EC-decay leads to a monoenergetic peak in the recoil energy spectrum at energy $E_{\mathrm{EC}} = Q^2/2 \cdot m_{\mathrm{i}}$, which is above the endpoint energy E_0 of the continuous recoil spectrum from β^+-decay. By measuring these EC-peaks for several suitable nuclides with different decay energies an energy calibration can be obtained. Furthermore, different charge states n produce EC-peaks at different energies E_{EC}/n for the same nuclide, which can also be used for energy calibration. The appearance of a peak also creates the possibility to detect EC-decay even at very low EC/β^+-branching ratios, which are common for β-decays with high Q-values.

3.4. Response function

The response function of the spectrometer has been investigated analytically as well as with simulations of the ion motion through the spectrometer. The analytic expression derives from a calculation based on the projection of the recoil momenta onto the radial direction, in which fully adiabatic conversion of the radial momenta according to Eq. (3) is assumed; it is furthermore assumed that all ions experience the same retardation potential. The resulting theoretical response function R for a monoenergetic peak at energy E' in the differential recoil energy spectrum is given by

$$R_{E,E'} \propto \sqrt{\frac{E'}{\sigma \cdot (E - (1-\sigma) \cdot E')}}, \quad (1-\sigma) \cdot E' < E \leqslant E' \tag{5}$$

and $R_{E,E'} = 0$ for all other E. In this equation σ is the energy resolution of the spectrometer and is given by $\sigma = B_{\min}/B_{\max} \approx 1.1\%$. Note that $\sigma \cdot E$ is the range of the response function at energy E and not its FWHM or standard deviation. This theoretical shape of the response function is shown in Fig. 6 (solid line).

The response function of the spectrometer has also been investigated via a numerical calculation of the ion trajectories as described in Section 2.2.2. It was obtained by repeating this calculation for different retardation voltages. As an example Fig. 6 (symbols) shows the response function for monoenergetic recoil ions that are emitted isotropically from an ion cloud in the center of the trap. This is compared to the analytical response function that assumes ideal adiabatic conversion from radial into axial energy and an ideal electric field in the analysis plane. As can be seen, the deviation of the simulated response function from the ideal response function is negligible, indicating that the motion of the recoil ions in the spectrometer is sufficiently adiabatic.

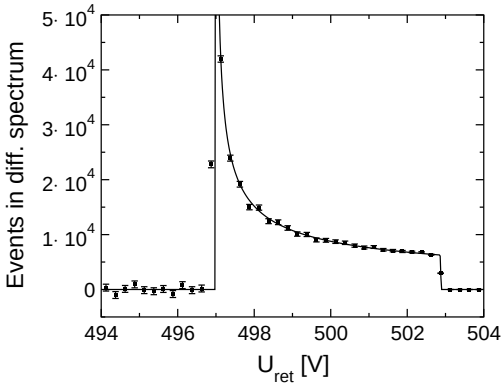

Fig. 6. Theoretical (solid line) and simulated (symbols, 6×10^5 events, $E = 503$ eV, $\sigma = 1.2\%$, see text) response functions. This is the line shape in the differential recoil energy spectrum. At $E \cdot (1 - \sigma)$ is a pole in the theoretical response function. The good agreement between the theoretical and simulated line-shape indicates that the ion motion will be sufficiently adiabatic for the field configurations used in the experiment.

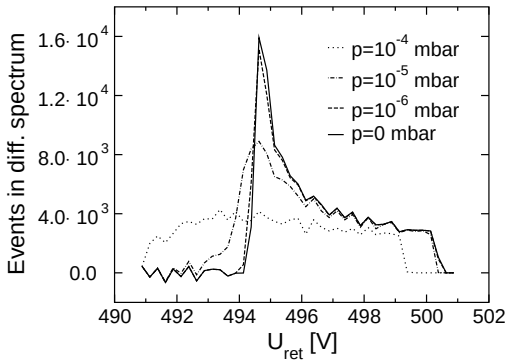

Fig. 7. Effect of the residual gas on the shape of the response function (for 1×10^7 events, $E = 500$ eV, $\sigma = 1.2\%$). The calculation was performed for argon buffer gas. For helium buffer gas the indicated pressures have to be multiplied by a factor of ≈ 0.1. In order to get a response function with a well-defined peak the residual gas pressure in the cooler trap needs to be $\leqslant 10^{-6}$ mbar or better.

The response function can be influenced by other effects like the space charge created by the trapped ions, nonadiabatic motion of the ions due to imperfections in the magnetic and electric fields, collisions of the ions in the decay trap with rest gas (Fig. 7), stray ions that decay in the spectrometer, etc. The influence of these and other as yet unknown effects will have to be investigated in detail experimentally.

The resolution of the spectrometer can be changed by varying the magnetic field strength in the low-field magnet. This magnet is designed for a maximum field strength of 0.2 T. The design of the spectrometer assumes a field strength of 0.1 T during the experiments, yielding the nominal resolution of $\sigma = 1.1\%$. The resolution can be improved by lowering the field strength in the low-field magnet. However, care has to be taken that when changing the magnetic field it still decreases monotonically between the decay trap and the analysis region. In order to achieve this the cryostat has been designed in a way that the distance between the two magnets can be changed by several *cm*. Decreasing the field in the low-field magnet may also lead to less adiabatic motion of the recoil ions of high mass or energy. It follows that the resolution can only be improved for a limited number of β-emitters.

3.5. Counting statistics

In order to determine the statistics achievable, the efficiencies inherent in the spectrometer design have to be considered. One trap load of N_1 ions stays for a time Δt in the decay trap. During this period a fraction

$$\varepsilon_{\Delta t} = 1 - \mathrm{e}^{-\ln 2(\Delta t/t_{1/2})} \tag{6}$$

of the ions will decay, where $t_{1/2}$ is their half-life. Assuming that the time to fill the decay trap is small compared to Δt, the number of trap loads in time t will be $t/\Delta t$ and the number of decays in the trap

$$N_t = \varepsilon_{\Delta t} \cdot N_1 \cdot \frac{t}{\Delta t}. \tag{7}$$

Not all of those recoil ions can be detected, though. Since only approximately half of the recoil ions are emitted into the spectrometer the solid angle reduces their number by $\varepsilon_\Omega \approx 0.5$. The first experiments will also be restricted to ions of charge state $n = 1$, which have a formation probability of $p_{(n=1)} = O(10\%)$ only. Finally, the detection efficiency of modern microchannel plate detectors is $\varepsilon_{\mathrm{MCP}} \approx 0.6$. Thus the number of ions that can be detected in time t is

$$N_{\mathrm{d}} = \varepsilon_\Omega \cdot \varepsilon_{\mathrm{MCP}} \cdot p_{(n=1)} \cdot N_t. \tag{8}$$

The WITCH experiment measures the cumulative recoil energy spectrum. For the measurement of each channel in the cumulative spectrum the same number of ions x has always to decay. These decays yield a number of x_i events in channel i, with $x_0 = x$ being the number of events for $U_{ret} = 0$. Since each channel in the differential spectrum is obtained from the difference of channels in the cumulative spectrum $N_i = x_{i-1} - x_i$ the number of events in the entire differential spectrum is $N = \sum_i N_i = x_0 = x$, assuming no energy-dependent background. The number of ions that have to decay in order to get these N events in the differential spectrum is correspondingly $N_d = (n_0 + 1) \cdot N$, where n_0 is the number of channels in the differential spectrum. Using Eqs. (6)–(8), the number of ions in the differential spectrum after time t is

$$N = \frac{\varepsilon_\Omega \cdot \varepsilon_{MCP} \cdot p_{(n=1)} \cdot (1 - e^{-\ln 2(\Delta t/t_{1/2})})}{(n_0 + 1) \cdot \Delta t} \cdot N_I \cdot t. \quad (9)$$

Typical numbers are $p_{(n=1)} = 0.1$, $\varepsilon_{MCP} = 0.6$, $\varepsilon_\Omega = 0.5$, $\Delta t = t_{1/2}$ and $N_I = 10^6$. Suitable isotopes for the initial measurements are, a.o., ^{35}Ar with $t_{1/2} = 1.8$ s and ^{26m}Al with $t_{1/2} = 6.3$ s.

Simulations show (Fig. 8) that the total number of events in the differential energy spectrum should be $N = 10^7$–10^8 and that a minimum of $n_0 = 20$ channels measured in the upper half of the spectrum seems to be sufficient to reach a precision of $\Delta a = 0.005$. The upper half of the spectrum contains only recoil ions with charge state $n = 1$, making it unnecessary to unfold different charge states. Using Eq. (9) and $N = 10^8$ the measurement time needed to achieve a precision of $\Delta a = 0.005$ is $t \approx 3$ days for ^{35}Ar and $t \approx 10$ days for ^{26m}Al. However, it needs to be pointed out that it should be feasible to increase the trap load by a factor of 10 to $N_I = 10^7$, which reduces the measurement time by the same factor.

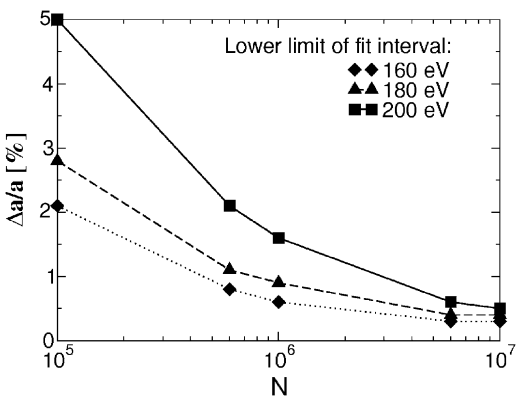

Fig. 8. Precision achievable on the β-ν angular correlation coefficient a (CL = 68.3%). This is the result of a simulation for $^{26}Al^m(E_0 = 280$ eV). Three curves are shown for different analysis intervals. The x-axis displays the number of events N in the total differential recoil energy spectrum. Typically, to get one differential event $\approx 10^4$ ions have to be trapped.

4. Status

The WITCH experiment is being set up at ISOLDE at present (spring 2003). The horizontal beamline (Fig. 2), which connects the WITCH set-up to the REXTRAP Penning trap and buncher, is fully operational. The vertical beamline with the pulsed drift tube and the deceleration electrodes is being installed. The cryostat with the two superconducting magnets has been delivered and was installed and successfully tested. Both the cooler trap and the decay trap exist and will be mounted still in the first half of 2003. The retardation electrodes are under construction. The microchannel plate detector for the recoil ions is currently mapped for the position dependence of its detection efficiency. Finally, the control system is under development; a first version of the core system will be available still in the first half of 2003. The experiment will be operational in summer 2003.

First tests with stable beam from REXTRAP have begun. Beam tuning into the high field region of the traps and first trapping tests will still start in the first half of 2003. It is planned to have radioactive beam of ^{35}Ar to measure a first recoil energy spectrum at the end of the ISOLDE beamtime in autumn 2003. A second beamtime is planned for spring 2004. The time in between the two measurements will be used to fix potential problems that may arise during the beamtime in 2003. These two beamtimes are intended to demonstrate that the WITCH experiment works in principle. Potentially a precision on the β-ν angular correlation coefficient a of 1% could be

reached with these first experiments, pending the investigation of systematic effects.

WITCH has been approved as ISOLDE test experiment P111 by the ISC[3] with 9 shifts of stable and 9 shifts of radioactive beam. Beyond this more beamtime will be needed to measure a recoil energy spectrum with high statistics and to investigate several systematic effects (calibration, normalization, response function, etc.).

5. Summary

The WITCH experiment will make it possible to measure the recoil energy spectrum of the daughter ions from nuclear β-decay with high precision. By combining a Penning trap with a retardation spectrometer these measurements can be performed for a wide variety of β-emitters. WITCH will thus be the first experiment where this recoil energy spectrum can be measured independent of the specific chemical, atomic or decay properties of the relevant isotope.

In a first step the WITCH experiment will be used to search for scalar and tensor weak interaction types. However, other research goals are also feasible with this set-up and will be discussed in a future article. Updates of the status of the experiment can be found in [47].

Acknowledgements

This work is supported by the European Union grants FMRX-CT97-0144 (the EUROTRAPS TMR network) and HPRI-CT-2001-50034 (the NIPNET RTD network), by the Flemish Fund for Scientific Research FWO and by the project GOA 99-02 of the K.U.Leuven. This research was partly funded with a specialization fellowship of the Flemish Institute for the stimulation of Scientific-Technological Research in the Industry (IWT). D.B. was supported by a Marie-Curie fellowship from the TMR program of the European Union. The authors want to thank J. Deutsch for discussions and invaluable suggestions.

[3] ISOLDE Scientific Committee, now INTC, ISOLDE and Neutron Time-of-flight Committee.

References

[1] P. Herczeg, Prog. Part. Nucl. Phys. 46 (2001) 413.
[2] N. Severijns, et al., Hyperfine Interactions 129 (2000) 223.
[3] E.G. Adelberger, et al., Phys. Rev. Lett. 83 (1999) 1299.
[4] A. Garcia, et al., Hyperfine Interactions 129 (2000) 237.
[5] W.C. Haxton, C.E. Wieman, Ann. Rev. Nucl. Part. Sc. 51 (2001) 261.
[6] C. Adloff, et al., Phys. Lett. B 523 (2001) 234.
[7] J.D. Jackson, S.B. Treiman, H.W. Wyld, Nucl. Phys. 4 (1957) 206.
[8] J.C. Hardy, et al., Nucl. Phys. A 509 (1990) 429.
[9] A.S. Carnoy, et al., Nucl. Phys. A 568 (1994) 265.
[10] I.S. Towner, J.C. Hardy, in: P. Herczeg, C.M. Hoffman, H.V. Klapdor-Kleingrothaus (Eds.), Proceedings of the Fifth International WEIN Symposium, Santa Fe, NM, USA, June 1998, World Scientific, Singapore 1999, p. 338.
[11] A.I. Boothroyd, et al., Phys. Rev. C 29 (1984) 603.
[12] C.S. Wu, S.A. Moszkowski, Beta Decay, Wiley, New York, 1966.
[13] T.D. Lee, C.N. Yang, Phys. Rev. 104 (1956) 254.
[14] C.H. Johnson, et al., Phys. Rev. 132 (1963) 1149.
[15] J.S. Allen, et al., Phys. Rev. 116 (1959) 134.
[16] L.S. Brown, G. Gabrielse, Rev. Mod. Phys. 58 (1986) 233.
[17] H.G. Dehmelt, Adv. At. Mol. Phys. 3 (1967) 53.
[18] J.D. Jackson, Classical Electrodynamics, Wiley, New York, 1962, p. 419.
[19] A. Picard, et al., Nucl. Instr. and Meth. B 63 (1992) 345.
[20] J. Bonn, et al., Nucl. Instr. and Meth. A 421 (1999) 256.
[21] V.M. Lobashev, P.E. Spivak, Nucl. Instr. and Meth. A 240 (1985) 305.
[22] O. Naviliat-Cuncic, private communication.
[23] E.L. Raab, et al., Phys. Rev. Lett. 59 (1987) 2631.
[24] A. Gorelov, et al., Hyperfine Interactions 127 (2000) 373.
[25] N.D. Scielzot, et al., Lawrence Berkeley National Laborator Nuclear Science Division Annual Report, 2001.
[26] E. Kugler, et al., Nucl. Instr. and Meth. B 70 (1992) 41.
[27] E. Kugler, Hyperfine Interactions 129 (2000) 23.
[28] D. Beck, et al., Letter of Intent to the ISOLDE committee, CERN/ISC 98-21, ISC/I 30, November 1998.
[29] D. Beck, et al., Proposal to the ISOLDE scientific committee, CERN/ISC 99-13, ISC/P111, April 1999.
[30] M. Beck, et al., Proceedings of the 14th International Conference on Electromagnetic Isotope Separators and Techniques Related to their Applications (EMIS 14), Victoria, Canada, May 2002, Nucl. Instr. and Meth. B, (2003) in press.
[31] B. Delauré, et al., at the Third Euroconference on Atomic Physics at Accelerators (APAC2001), Aarhus, Denmark, September 2001, Hyperfine Interactions, (2003) to be published.

[32] M. Beck, et al., in: Z. Parsa, W.J. Marciano (Eds.), Proceedings of the 7th Conference on the Intersection of Particle and Nuclear Physics, Quebec City, Canada, May 2000, A.I.P. Conf. Proc., Vol. 549, 2000, p. 934.
[33] D. Beck, et al., Proceedings of the Radioactive Nuclear Beams (RNB) 2000 Conference, Divonne, France, April 2000, Nucl. Phys. A 701 (2002) 369c.
[34] M. Beck, et al., in: K. Cheung, J.F. Gunion, S. Mrenna (Eds.), Proceedings of the 7th International Symposium on Particles, Strings and Cosmology (PASCOS), Granlibakken, Lake Tahoe, CA, December 1999, World Scientific, Singapore 2000, p. 544.
[35] D. Beck, et al., Proceedings of the International Workshop on Trapped Particles and Fundamental Physics, Monterey, CA, U.S.A., 31 August–04 September 1998, A.I.P. Conference Proceedings, Vol. 457, 1999, p. 172.
[36] F. Ames, et al., Proceedings of the Exotic Nuclei and Atomic Masses, Bellaire, USA, 1998, A.I.P. Conference Proceedings, Vol. 445, 1998, p. 927.
[37] F. Herfurth, et al., Nucl. Instr. and Meth. A 469 (2001) 254.
[38] D. Lunney, G. Bollen, Hyperfine Interactions 129 (2000) 249.
[39] H. Raimbault-Hartman, et al., Nucl. Instr. and Meth. B 126 (1997) 378.
[40] G. Bollen, et al., Nucl. Instr. and Meth. A 368 (1996) 675.
[41] H. Schnatz, et al., Nucl. Instr. and Meth. A 251 (1986) 17.
[42] G. Savard, et al., Phys. Lett. A 158 (1991) 247.
[43] D. Beck, et al., Hyperfine Interactions 132 (2001) 473.
[44] B. Brehm, et al., Meas. Sci. Technol. 6 (1995) 953.
[45] W.H. Press, et al., Numerical Recipes, Cambridge University Press, Cambridge, 1996.
[46] A.H. Snell, The atomic and molecular consequences of radioactive decay, in: Siegbahn (Ed.), Alpha-, Beta- and Gamma-Ray Spectroscopy, North-Holland, Amsterdam, 1968, p. 1545.
[47] http://www.fys.kuleuven.ac.be/iks/ko/research/witch/default.htm